International Journal of Electrical, Electronic and Communication Sciences
ISSN: 2517-9438
Vol:7, No:6, 2013

Development of a Real-Time Energy Models for Photovoltaic Water Pumping System

Ammar Mahjoubi, Ridha Fethi Mechlouch, Belgacem Mahdhaoui, and Ammar Ben Brahim

***Abstract*—**This purpose of this paper is to develop and validate a model to accurately predict the cell temperature of a PV module that adapts to various mounting configurations, mounting locations, and climates while only requiring readily available data from the module manufacturer. Results from this model are also compared to results from published cell temperature models. The models were used to predict real-time performance from a PV water pumping systems in the desert of Medenine, south of Tunisia using 60-min intervals of measured performance data during one complete year. Statistical analysis of the predicted results and measured data highlight possible sources of errors and the limitations and/or adequacy of existing models, to describe the temperature and efficiency of PV-cells and consequently, the accuracy of performance of PV water pumping systems prediction models.

***Keywords*—**Temperature of a photovoltaic module, Predicted models, PV water pumping systems efficiency, Simulation, Desert of southern Tunisia.

I. Introduction

PHOTOVOLTAIC (PV) cell is one of the most popular renewable energy products. It can directly convert the solar radiation into electricity which can be utilised to power different systems, for example PV water pumping systems. However, the high cost of solar cells is an obstacle to expansion of their use. This is because during the operation of the PV cell, only around 15% of solar radiation is converted to electricity with the rest converted to heat. The electrical efficiency will decrease when the operating temperature of the PV module increases.

Many research efforts have focused on the development of empirical models that are able to predict photovoltaic water pumping system performance for any climatic condition using various parameters.

Many cell temperature models are available in literature. Details of a sampling of these models are included in the next section. These models can be generally grouped into three categories: empirical models, semi-empirical models, and theoretical models.

In this paper, a general energy balance model was developed to predict the cell temperature of a PV module. This model was simplified and validated using field measurements into a steady state model.

The objective of this paper therefore, is, to develop a validated real-time mathematical model that predicts the cell temperature of a PV module. The model can be used to generate the performance of PV water pumping systems.

A. Mahjoubi is with the National School of Engineering of Gabes, University of Gabes, Gabes 6029 TUNISIA (corresponding author: phone: 00216-97862751; fax: 00216-75600632; (e-mail: mahjoubiammar@yahoo.fr).
R. F. Mechlouch is with the National School of Engineering of Gabes, University of Gabes, Gabes 6029 TUNISIA (e-mail: mechlouch@yahoo.fr).
B. Mahdhaoui is with the National School of Engineering of Gabes, University of Gabes, Gabes 6029 TUNISIA (e-mail: mahdaouib@gmail.com).
A. Ben Brahim is with the National School of Engineering, University of Gabes, Gabes 6029 TUNISIA (e-mail: ammar.benbrahim@enig.rnu.tn).

II. Modeling of the Performances of a PV Water Pumping Systems

A. PV-Cell Temperature

Many PV cell temperature (T_c) models are available in literature. Details of a sampling of these models are included below. These models can be generally grouped into three categories: empirical models, semi-empirical models, and theoretical models.

Empirical models are developed purely from experimental data. Empirical models have the possibility to be very accurate since they are developed from actual data and do not need to make assumptions. The downside is the fact that, since the model requires measured data, it is difficult to predict the performance of a module before installation.

King et al. have developed in [1] an empirical model for three mounting types that is dependent on irradiance, wind speed, and ambient temperature. In [2] a cell temperature model for the interior modules in a gap mounted rooftop array is developed by Shresta et. al.

Theoretical models apply established heat transfer correlations to predict the temperature of the module. As opposed to empirical models, theoretical models do not require measured performance. Fuentes developed an extensive transient model [3] that is adaptable to different mounting using equations manipulating the reported Nominal Operating Cell Temperature (NOCT). Jones and Underwood [4] developed a transient model for a rack mounted module, while Davis et al. [5] developed a transient model for a building integrated module. Duffie and Beckman [6] presented a simplified steady state model that adapts to the mounting of the module using the reported NOCT.

Semi-empirical models are defined as theoretical models that are slightly modified by information from experimental data. For example, Del Cueto [7] empirically calculates coefficients to improve a theoretical steady state model. Krauter et al. [8] developed a semi-empirical transient model. Skoplaki et al. [9] developed a simplified steady state model and modified the temperature for mounting conditions based on an empirical mounting coefficient.

In addition to previous models, Skoplaki and Palyvos [10] list additional cell temperature models. They include explicit and implicit models.

The explicit correlation models express the PV-cell temperature (T_c) as a function of ambient temperature, solar radiation, wind speed and other system parameters ignoring heat exchange dynamics between the module and its environment. Several equations for T_c found in the literature are listed in Table I.

TABLE I
EXPLICIT CORRELATIONS OF PV-CELL TEMPERATURE

Models	N°
$T_c = T_a + [(\alpha - \eta)G_T + (a + bT_a)]/(17.8 + 2.1V_w)$	(E.1)
$T_c = T_a + \alpha G_T(1 + \beta T_a)(1 - \gamma V_w)(1 - 1.053\eta_c)$	(E.2)
$T_c = T_a + G_T(\frac{\tau\alpha}{U_L})[1 - (\frac{\eta_c}{\tau\alpha})]$	(E.3)
$T_c = T_a + G_T\frac{(\tau\alpha - \eta_c)}{U_L}$	(E.4)
$T_c = T_a + \frac{G_T}{C_1 + C_1V_w}[(1-\rho)(1-\eta) - \sigma\frac{\varepsilon T_c^4 - T^4_{sky}}{G_T}$	(E.5)
$T_c = T_a + \frac{G_T}{G_{NOCT}}(T_{c,NOCT} - T_a)(1 - \frac{\eta_c}{\tau\alpha})$	(E.6)
$T_c = T_a + \frac{G_T}{G_{NOCT}}(T_{c,NOCT} - T_{a,NOCT})(1 - \frac{\eta_c}{\tau\alpha})$	(E.7)
$T_c = T_a + G_T(\frac{\alpha}{U_L})[1 - (\frac{\eta_c}{\alpha})]$	(E.8)
$T_c = T_a + (\frac{G_T}{G_{NOCT}})(\frac{U_{L,NOTC}}{U_L})(T_{NOCT} - T_{a,NOCT})[1 - (\frac{\eta_c}{\tau\alpha})]$	(E.9)
$T_c = T_a + (\frac{9.5}{5.7 + 3.8V_w})(\frac{G_T}{G_{NOCT}})(T_{NOCT} - T_{a,NOCT})[1 - (\frac{\eta_c}{\tau\alpha})]$	(E.10)
$T_{bs} = \frac{h_{p1}(\tau\alpha)_{eff}G_T + U_{tb}T_a + h_bT_w}{U_{tb} + h_b}$	(E.11)
$T_c = \frac{\tau[\alpha_c p + \alpha_T(1 - \beta_c)]G_T - \eta_c\beta_cG_T + U_tT_a + U_tT_{bs}}{U_t + U_{Ta}}$	(E.12)
$T'_c = \frac{\tau[\alpha_c p + \alpha_T(1 - \beta_c)]G_T + (U_t + U_{Ta})T_a}{U_t + U_{Ta}}$	(E.13)

The implicit correlations, i.e. involve variables such as cell efficiency or heat transfer coefficients, which themselves depend on T_c. Some implicit correlations are shown in Table II.

TABLE II
IMPLICIT CORRELATIONS OF PV-CELL TEMPERATURE

Models	N°
$T_c = 3.12 + 0.025G_T + 0.899T_a - 1.30V_w)$	(E.14)
$T_c = 3.81 + 0.0282G_T + 1.31T_a - 1.65V_w$	(E.15)
$T_c = [\frac{(U_0/F_p)(m_0/F_p)(T_a + T_{c0})}{2(m_0/F_p)}][(1+Y)^{1/2} - 1]$	(E.16)
$T_c = T_a + 0.028G_T - 1.0$	(E.17)
$T_c = T_a + 0.035G_T$	E.18)
$T_c = T_a + \alpha G_T(1 + \beta T_a)(1 - \gamma V_w)$	(E.19)
$T_c = \frac{T_a + [\alpha_{cell} - \eta_{ref}(1 + \beta T_{ref})](\frac{G_T}{h})}{1 - \eta_{ref}\beta(\frac{G_T}{h})}$	(E.20)
$T_c = \frac{[\tau\alpha - \eta_{ref}]G_T + T_a[h_{cf} + 2\sigma\varepsilon_c\tau_{IR}(1+\cos\beta)T_{sky}T^2{}_a + h_{cb} + 4\sigma T^3{}_aF_eF_b]}{h_{cf} + 2\sigma\varepsilon_c\tau_{IR}T^3{}_a(1+\cos\beta) + h_{cb} + 4\sigma T^3{}_aF_eF_b}$	(E.21)
$T_c = T_a + 0.0155G_T + 0.7$	(E.22)
$T_c = 30 + 0.0175(G_T - 150) + 1.14(T_a - 25)$	(E.23)
$T_c = T_a + \frac{G_T}{G_{NOCT}}[0.0712V^2{}_w - 2.411V_w + 32.96]$	(E.24)
$T_c = T_a + (\frac{G_T}{G_{NOCT}})(T_{c,NOCT} - T_{a,NOCT}) = T_a + \frac{G_T}{800}(NOCT - 20)$	(E.25)
$T_c = T_a + (219 + 832\overline{K}_t)\frac{NOCT - 20}{800}$	(E.26)
$T_c = 30 + 0.0175(G_T - 150) + 1.14(T_a - 25)$	(E.27)
$T_c = T_i + K\eta_TG_T, K = \frac{1 - F_R}{F_RU_L}$	(E.28)
$T_c = T_a + \frac{G_T}{G_{Tref}}[T_1e^{bV_w} + T_2 + \Delta T_{ref}]$	(E.29)

$$T_c = T_a + G_T[e^{(a+bV_F)} + \frac{\Delta T_{ref}}{G_{T\,ref}}] \quad (E.30)$$

$$T_c = T_a + 0.031 G_T \quad (E.31)$$

$$T_c = T_a + 0.031 G_T - 0.058 \quad (E.32)$$

B. Steady-State Analysis

A general energy balance model was developed to predict the cell temperature of PV module. This model was simplified and validated using field measurements into a steady state model that creates a thermal resistance network between the cell and the ends of the module. Fig. 1 gives a schematic of the thermal energy exchanges between PV module and the environment, which involve such variables and parameters.

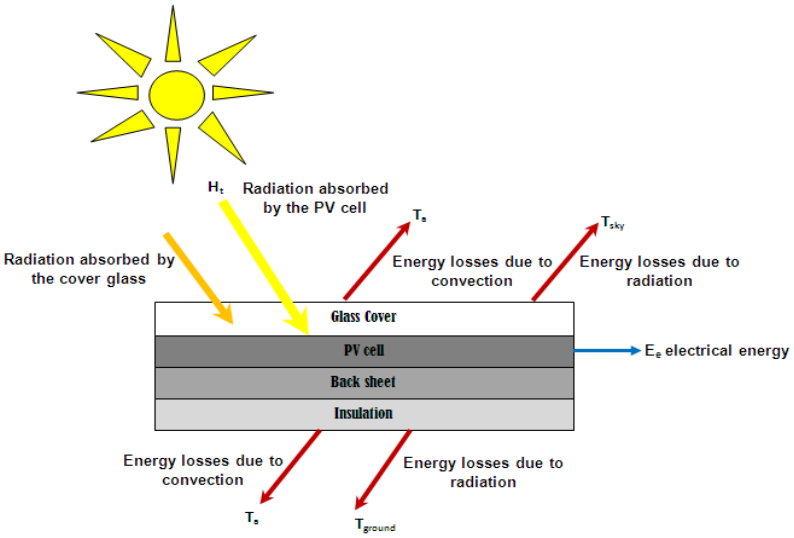

Fig. 1 Simple schematic of the thermal processes in PV module

The equation for the PV-cell temperature operating under steady state is derived assuming that the incident energy on a solar cell is equal to the electrical energy output of the cell plus the sum of the energy losses due to convection and radiation. The resulting energy balance equation is given as [11]-[12]:

$$\dot{Q}_H = E_e + \dot{Q}_{rad} + \dot{Q}_{conv} \quad (1)$$

where: $$\dot{Q}_H = \tau\alpha H_t A \quad (2)$$

where:α: absorptivity and τ : transmissivity.

E_e is the electrical energy produced by the module, where

$$E_e = \eta_p H_t A \quad (3)$$

$$\dot{Q}_{ray} + \dot{Q}_{conv} = U_P A(T_c - T_a) \quad (4)$$

$U_P = h_{rad} + h_{conv}$: Thermal losses by radiation and thermal losses by convection.

where: $$h_{rad} = \varepsilon\sigma(T_{sky} + T_c)(T_{sky}^2 + T_c^2) \quad (5)$$

$$h_{conv} = 5{,}82 + 4{,}07V_w \quad (6)$$

where: ε and σ are respectively emissivity and Stefane Boltzman's constant, V_w is the wind speed.

The effective temperature of the sky (T_{sky}) is calculated from the following empirical relation:

$$T_{sky} = T_a - 6 \quad (7)$$

Substituting the relevant terms in Eq. (1) results in Eq. (8) given as:

$$\tau\alpha H_t = \eta_p H_t + U_P(T_c - T_a) \quad (8)$$

Finally, the PV-module temperature is given as:

$$T_c = \frac{H_t}{\varepsilon\sigma(T_{sky} + T_c)(T_{sky}^2 + T_c^2) + (2{,}8 + 3V_w)}(1 - \frac{\eta_p}{\tau\alpha}) + T_a \quad (9)$$

C. Description of the Algorithm

The performance of PV water pumping system is simulated using MATLAB 7 software with an hourly time step. The program is based on the proposed models for calculation of hourly water flow rate. This simulation program uses the hourly global solar radiation, the hourly ambient temperature and the hourly wind speed as the input, moreover the characteristics of region (Latitude, Longitude, ground albedo) and characteristics of photovoltaic water pumping system (orientation, inclination, NOCT, PV array area, temperature of reference, HMT,...).

The first step consists of the determination of the various astronomical parameters, and more precisely the exact position of the sun at any moment of the year.

The first parameter to be determined is the declination; it is the angular position of the sun at solar noon, with respect to the plane of the equator. Its value in degrees is given by Cooper's equation [13]:

$$\delta = -23.45\mathrm{Sin}\left[\frac{360(284+q)}{365.25}\right] \tag{10}$$

where q is the day of year (i.e. q =1 for January 1, q = 32 for February 1, etc.). Declination varies between -23.45° on December 21 and +23.45° on June 21.

The stage which comes then is the calculation of the true solar time (TSV):

$$\mathrm{TSV} = \mathrm{H}_{\mathrm{Greenwich}} + \frac{\lambda}{15} + Et \tag{11}$$

where λ is the longitude of the site and Et is the equation of time;

$$Et = \left[9.87Sin(2B) - 7.5\,\mathrm{Cos}B - 1.5\,\mathrm{Sin}B\right]\frac{1}{60} \tag{12}$$

$$\mathrm{B} = \left[\frac{360(\mathrm{q}-81)}{365}\right] \tag{13}$$

The solar hour angle is the angular displacement of the sun east or west of the local meridian; morning negative, afternoon positive.

$$\omega = 15\left(\mathrm{TSV} - 12\right)\frac{\pi}{180} \tag{14}$$

The sunset hour angle ω_0 is the solar hour angle corresponding to the time when the sun sets.

It is given by the following equation:

$$\omega_0 = \mathrm{a}rc\cos\left(-\tan\varphi.\tan\delta\right) \tag{15}$$

where δ is the declination, calculated through equation (10), and φ is the latitude of the site, specified by the user.

The zenith angle of the sun θ_z is calculated through this equation:

$$\mathrm{Cos}\,\theta_z = \mathrm{Sin}\,\delta.\mathrm{Sin}\,\varphi + \mathrm{Cos}\,\delta\,.\mathrm{Cos}\,\varphi.\mathrm{Cos}\,\omega \tag{16}$$

The hourly extraterrestrial radiation on a horizontal surface, H_0, can be computed for hour from the following equation [13]:

$$H_0 = \frac{24}{\pi}.\mathrm{I}_0\left(1+0{,}033\times\cos\left(\frac{\mathrm{q}\times360}{365}\right)\right)\left[Cos\varphi.Cos\delta.Sin\omega_0 + \frac{2\pi.\omega_0}{360}.Sin\varphi.Sin\delta\right] \tag{17}$$

The ratio of global solar radiation at the surface of the earth to extraterrestrial radiation is called the clearness index. Thus the hourly clearness index, K_T, is defined as:

$$K_T = \frac{\mathrm{H}}{H_0} \tag{18}$$

The fraction diffuse is the ratio of the diffuse solar radiation to the global solar radiation [14]:

$$f_d = \frac{\mathrm{H_d}}{H} \tag{19}$$

$f_d = 1 - 0.09\mathrm{K_T}$ for $0 <= \mathrm{K_T} <= 0.22$ (20)

$f_d = 0.9511 - 0.1604\mathrm{K_T} + 4.388\mathrm{K_T}^2 - 16.638\mathrm{K_T}^3 + 12.336\mathrm{K_T}^4$ for $0.22 < \mathrm{K_T} <= 0.8$ (21)

$f_d = 0.1$ for $\mathrm{K_T} > 0.8$ (22)

Where the diffuse solar radiation H_d, is defined as:

$$\mathrm{H_d} = f_d.H \tag{23}$$

After calculation of diffuse radiation, the direct radiation is obtained just by difference with global solar radiation which can be expressed as:

$$\mathrm{H_b} = H - H_d \tag{24}$$

Calculation of hourly irradiance in the plane of the PV array, H_t [13]:

$$H_t = H_b.R_b + H_d.(\frac{1+\cos\beta}{2}) + H.\alpha'.(\frac{1-\cos\beta}{2}) \tag{25}$$

where α represents the diffuse reflectance of the ground (also called ground albedo is set to 0.2) and β represents the slope of the PV array (inclination).

R_b is the ratio of beam radiation on the PV array to that on the horizontal, which can be expressed as:

$$R_b = \frac{\cos\theta}{\cos\theta_z} \tag{26}$$

where θ is the incidence angle of beam irradiance on the array and γ is the orientation of the PV array.

$$\begin{aligned}\mathrm{Cos}\theta &= \mathrm{Sin}\delta.\mathrm{Sin}\varphi.Cos\beta - Cos\varphi.Sin\delta.Sin\beta.\mathrm{Cos}\gamma \\ &+ \mathrm{Cos}\delta.\mathrm{Cos}\varphi.\mathrm{Cos}\beta.\mathrm{Cos}\omega + \mathrm{Sin}\varphi.Cos\delta.Sin\beta.\mathrm{Cos}\gamma.\mathrm{Cos}\omega \\ &+ Cos\delta.Sin\beta.Sin\gamma.\mathrm{Sin}\omega\end{aligned} \quad (27)$$

The energy delivered by the PV array, Ee, is simply [15]:

$$E_e = S\,\eta_p\,H_t\,(1-\lambda_p)(1-\lambda_c) \quad (28)$$

where S is the area of the array. It has to be reduced by miscellaneous PV array losses λ_p and other power conditioning losses λ_c:

The array is characterized by its average efficiency, η_p, which is a function of average module temperature T_c:

$$\eta_p = \eta_r\,[1-\beta_p\,(T_c - T_r)] \quad (29)$$

where η_r is the PV module efficiency at reference temperature T_r (= 25°C), and β_p is the temperature coefficient for module efficiency.

T_c is related to the hourly ambient temperature T_a through formula (9):

$$T_c = \frac{H_t}{\varepsilon\sigma(T_{sky}+T_c)(T_{sky}^2+T_c^2)+(2{,}8+3V_w)}\left(1-\frac{\eta_p}{\tau\alpha}\right)+T_a$$

where NOCT is the Nominal Operating Cell Temperature, K_T the hourly clearness index and β_{opt} is the optimum tilt angle and β is the actual tilt angle.

The water pumping model is based on the simple equations [16]. The hourly hydraulic energy demand E_{hydr} (Wh), corresponding to lifting water to a height h (m) with a hourly volume Q (m^3/h) is:

$$E_{Hydr} = \rho.g.Q\left(1+\eta_f\right) = \rho.g.Q.HMT \quad (30)$$

where g is the acceleration of gravity (9.81 $m.s^{-2}$), ρ is the density of water (1000 $kg.m^{-3}$), and η_f is a factor accounting for friction losses in the piping. This hydraulic energy translates into an electrical energy requirement Ee:

$$E_e = \frac{E_{Hydr}}{R_p} = \frac{\rho.g.Q.HMT}{R_p} \quad (31)$$

where R_p is the pump system efficiency. If the pump is AC, this equation has to be modified to take into account the inverter efficiency R_{inv}:

$$E_e = \frac{\rho.g.Q.HMT}{R_p.R_{inv}} \quad (32)$$

Equalizing the two equations (28) and (32),

$$E_e = \frac{\rho.g.Q.HMT}{R_p.R_c} = S\,\eta_p\,H_t\,(1-\lambda_p)(1-\lambda_c) \quad (33)$$

The hourly volume pumping (flow rate) Q (m^3/h), which can be expressed as:

$$Q = \frac{S\,\eta_p\,H_t\,(1-\lambda_p)(1-\lambda_c).R_p.R_c}{\rho.g.HMT} \quad (34)$$

III. Description of the PV Water Pumping Systems

In this work, two solar water pumping stations are selected. These stations are located in the isolated site in Medenine city (south of Tunisia); with a Saharan climate. The first station named Bel Khchab (33.10 N, 10.05 E) and the second station named Om Chraket (32.55 N, 11.33 E). The two systems are used for potable water. A PV water pumping system consists of a PV array, inverter, submersible pump, storage tank, and auxiliary system of measuring devices and weather monitoring sensors, the two station work without storage batteries.

The Photographs and characteristics of the PV pumping stations are shown respectively in Fig. 2 and Table III.

(a)

(b)

Fig. 2 Photographs of stations Bel Khchab (a) and Om Chraket (b)

TABLE III
Characteristics of the PV Water Pumping Stations

Station	Bel Khchab	Om Chraket
Modules	monocrystal (100Wc, 24V)	monocrystal (65Wc, 12V)
PV array area (m^2)	85	21
Nominal PV module efficiency (%)	14	14
Miscellaneous PV array losses (%)	5	5

Miscellaneous power conditioning losses (%)	2	2
Moto-Pump	Grundfos SP 8A-44 (7.5 kWh)	Grundfos SP 3A-10 (1.2 kWh)
Pump system efficiency (%)	45	45
Inverter	Telemecanique DC/AC	Grundfos SA-1500 DC/AC
Inverter efficiency (%)	90	90
HMT	100 m	40 m
Capacity storage tank	500 m^3	20 m^3
PV temperature coefficient (%/°C)	0.4	0.4
NOCT(°C)	47	47
Temperature of reference (°C)	25	25

The modules in two stations are mounted on a supporting structure so that the surface azimuth angle and the inclination angle of the modules are zero and 35°, respectively.

The data acquisition system used in these stations is designed and made by us [17].

The proposed system consists of a set of sensors (can record up to 15 different sensors) for measuring both meteorological (e.g. solar irradiance, temperature etc.) and photovoltaic parameters (water flow rate, PV voltage and current etc.).

The experimental data is registered in a data logger located about 150 km from the CRDA of Medenine. The information from the data logger will be transmitted to the PC at anytime via GSM modem, where they are processed using the data acquisition software. The data acquisition software is used to further process, display and store the collected data in the PC disk. Fig. 3 shows the interface of data acquisition software.

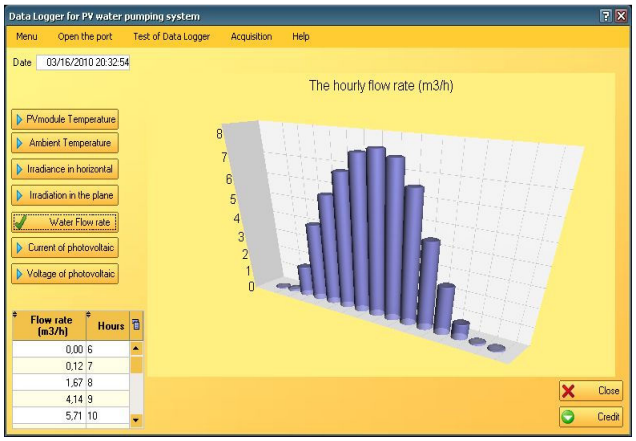

Fig. 3 Interface of data acquisition software

The pumped water flow rate is the principal measuring parameter, the ambient temperature, global irradiation on an inclined and horizontal surface (H_t, H), voltage and current of photovoltaic field (V, I) are also measured in order to construct a complete data base of the site and the system. The following transducers have been used for the various measurements. Turbine flow meters have been used for the flow rate measurements. The flow meters work in the range of 0 to 10 m^3/h with an accuracy of ±0.05%. The flow meters give 4:20 mA analog signal calibrated to the measured flow rate. Silicon pyranometers have been used to measure the solar radiation in the horizontal plane and in the plane of the PV arrays. The accuracy of the pyranometers is 10 W/m^2 or ±5%. Ambient temperature has been measured using an RTD sensor shielded from the sun. The uncertainty in the measurement of temperature is ±0.5°C. The DC voltage and current generated by the PV arrays and the AC voltage and current drawn by the pump motors have been measured using Hall Effect transducers of appropriate ranges. The accuracy of the voltage and current transmitters is ±0.25% of full scale.

The experimental data registered in a data logger during one complete year (2010) at a time interval of one hour and transmitted from remote photovoltaic water pumping systems in the desert of Tunisia to the PC are analyzed.

The mean monthly global solar radiations measured in the horizontal surface of Medenine city are plotted in Fig. 4. From this figure, we find that the maximum monthly mean of global radiation occurs in summer 289 kWh/m² per month and in spring 261 kWh/m² per month. In autumn and winter we find respectively 197 kWh/m² per month and 153 kWh/m² per month.

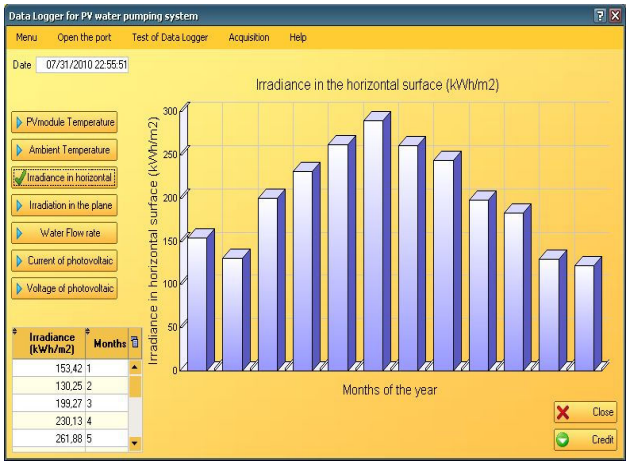

Fig. 4 Variation of mean monthly irradiance measured in horizontal surface of the year 2010 for Medenine

The mean monthly irradiance measured in the plane of the PV array of Medenine city is plotted in Fig. 5. We find that the maximum of global solar radiation is high throughout the summer months reaching 281 kWh/m² per month, in spring month's 274 kWh/m² per month. In autumn and winter we find respectively 208 kWh/m² per month and 171 kWh/m² per month. Another factor which is prejudicial to the good behavior and the efficiency of the PV array is the ambient temperature. We can see in Fig. 6, the monthly average variations of the ambient temperature of the year 2010. Temperatures can be very high and reach 44°C, especially in the period stretching from May to September.

The areas of the desert of Medenine, in the South of Tunisia, benefit from a very significant irradiation for which the use of PV water pumping system can be considered with strong chances of success.

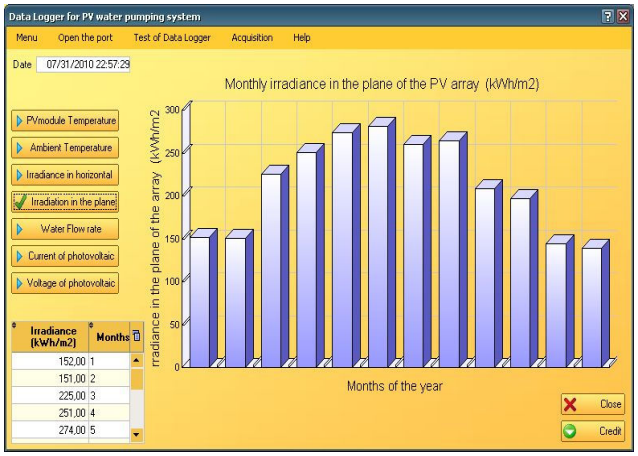

Fig. 5 Variation of mean monthly irradiance measured in the plane of the PV array of the year 2010 for Medenine

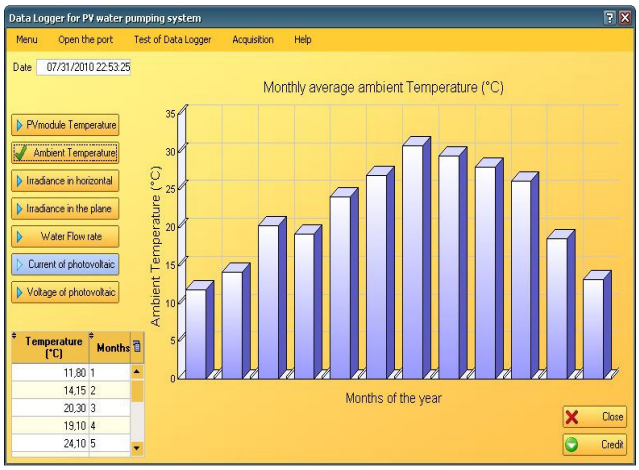

Fig. 6 Measured monthly average ambient temperature of the year 2010 for Medenine

IV. Results and Discussion

In order to quantify variations between predicted and measured values, root mean square error (RMSE) was used. It evaluates the percentage mean of the sum of absolute deviations arising due to both over-estimation and under-estimation of individual observations. RMSE is given as:

$$RMSE = \left(\frac{\sum \left(X_{mC} - X_{mD} \right)^2}{N} \right)^{\frac{1}{2}} \quad (35)$$

N is the total number of observations while X_{mC} and X_{mD} are the i_{th} calculated and measured values, respectively.

A. PV-Cell Temperature

Table IV presents RMSE for PV-cell temperature predictions using the present model, Model of Durisch et al. and the Model of Kou et al. (respectively the models in Eqs. (9), (E.6) and (E.18). The results show that the empirical models in Eqs. (9), (E.6) and (E.18) produce the least RMSE of 2.6%, 5.4% and 5.7%, respectively. Where field trial data is not available to derive the empirical coefficients, Eq. (9) can be used to predict the PV-cell temperature with a higher RMSE of 2.6%.

TABLE IV
Root Mean Square Error (RMSE) for PV-Cell Temperature Predictions

PV-cell temperature models	RMSE (%)
Present model/Measured	2.6
Model of Durisch et al./Measured	5.4
Model of Kou et al./Measured	5.7

Fig. 7 shows plots of measured and modeled PV-cell temperature using Eqs. (9), (E.6) and (E.18). It can be seen from Fig. 7 that the predicted PV-cell temperatures show good correlation with the measured data.

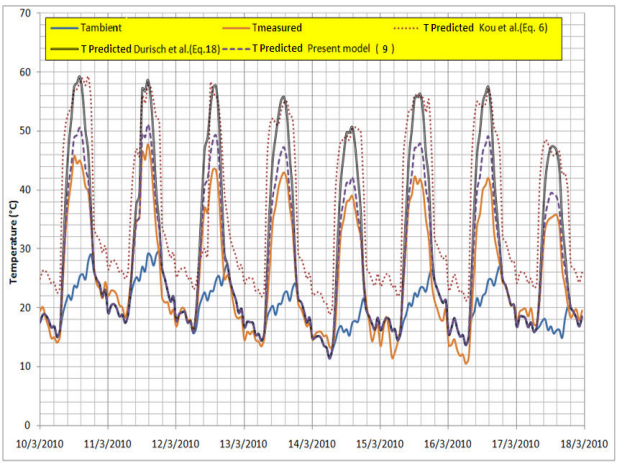

Fig. 7 Measured and modeled PV-cell temperature

B. PV Water Pumping System Performance

Table V and VI show the predict results obtained for the PV water pumping system PVWPS (Station Bel Khchab) for four days during the month of January, March, July and October, respectively.

TABLE V
Predicted Performance Using Simulation Model in January 1th, 2010 (Station Bel Khchab)

Hours	K_T	H_t (kWh/m^2)	Ee (kWh)	Q (m^3/h)
6	0.00	0.000	0.00	0.00
7	0.00	0.000	0.00	0.00
8	0.44	0.030	0.02	0.03
9	0.27	0.101	0.39	0.58
10	0.74	0.452	4.88	4.05
11	0.46	0.469	2.08	4.09
12	0.23	0.309	0.86	2.28

13	0.22	0.287	0.85	1.98
14	0.22	0.258	0.81	1.69
15	0.29	0.221	0.95	1.41
16	0.35	0.190	0.90	1.33
17	0.38	0.103	0.65	0.97
18	0.00	0.020	0.01	0.02
19	0.00	0.000	0.00	0.00
20	0.00	0.000	0.00	0.00
Daily water flow rate m^3/day				18.43

TABLE VI
PREDICTED PERFORMANCE USING SIMULATION MODEL IN MARCH 16TH, 2010 (STATION BEL KHCHAB)

Hours	K_T	H_t (kWh/m^2)	Ee (kWh)	Q (m^3/h)
6	0.00	0.00	0.00	0.00
7	0.00	0.00	0.08	0.12
8	0.44	0.00	1.12	1.67
9	0.27	0.05	2.79	4.14
10	0.74	0.65	3.84	5.71
11	0.46	0.27	4.60	6.83
12	0.23	0.11	5.17	7.68
13	0.22	0.11	5.32	7.91
14	0.22	0.10	5.15	7.65
15	0.29	0.12	4.45	6.61
16	0.35	0.11	3.04	4.51
17	0.38	0.08	1.71	2.54
18	0.00	0.00	0.57	0.84
19	0.00	0.00	0.05	0.08
20	0.00	0.00	0.00	0.00
Daily water flow rate m^3/day				56.31

TABLE VII
PREDICTED PERFORMANCE USING SIMULATION MODEL IN JULY 15TH, 2010 (STATION BEL KHCHAB)

Hours	K_T	H_t (kWh/m^2)	Ee (kWh)	Q (m^3/h)
6	0.00	0.00	0.29	0.43
7	0.00	0.00	0.63	0.94
8	0.44	0.00	1.09	1.62
9	0.27	0.05	2.24	3.32
10	0.74	0.65	3.22	4.79
11	0.46	0.27	4.08	6.07
12	0.23	0.11	4.56	6.78
13	0.22	0.11	4.69	6.97
14	0.22	0.10	4.46	6.63
15	0.29	0.12	3.98	5.91
16	0.35	0.11	3.12	4.63
17	0.38	0.08	2.00	2.97
18	0.00	0.00	0.89	1.33
19	0.00	0.00	0.15	0.23
20	0.00	0.00	0.00	0.00
Daily water flow rate m^3/day				52.61

TABLE VIII
PREDICTED PERFORMANCE USING SIMULATION MODEL IN OCTOBER 15TH, 2010 (STATION BEL KHCHAB)

Hours	K_T	H_t (kWh/m^2)	Ee (kWh)	Q (m^3/h)
6	0.00	0.00	0.16	0.23
7	0.00	0.00	1.10	1.64
8	0.44	0.00	2.27	3.37
9	0.27	0.05	3.26	4.85
10	0.74	0.65	3.99	5.93
11	0.46	0.27	4.36	6.49
12	0.23	0.11	5.26	7.81
13	0.22	0.11	5.66	8.42
14	0.22	0.10	5.04	7.50
15	0.29	0.12	3.45	5.13
16	0.35	0.11	1.41	2.10
17	0.38	0.08	0.09	0.14
18	0.00	0.00	0.00	0.00
19	0.00	0.00	0.00	0.00
20	0.00	0.00	0.00	0.00
Daily water flow rate m^3/day				53.59

Table IX shows the predict results obtained for the PV water pumping system (Station Om Chraket) for four days during the month of January, March, July, and October, respectively.

TABLE IX
PREDICTED PERFORMANCE IN JANUARY 1TH, MARCH 16TH, JULY 15TH, OCTOBER 15TH, 2010 (STATION OM CHRAKET)

Hours	January 1th	March 16th	July 15th	October 15th
	Q (m^3/h)			
6	0.00	0.00	0.00	0.14
7	0.00	0.07	0.25	0.96
8	0.02	0.98	0.55	1.98
9	0.44	2.44	0.95	2.85
10	1.78	3.36	1.96	3.49
11	1.89	4.02	2.82	3.82
12	1.68	4.52	3.57	4.59
13	1.42	4.66	3.99	4.95
14	1.19	4.50	4.10	4.41
15	0.98	3.89	3.90	3.02
16	0.86	2.65	3.48	1.24
17	0.57	1.50	2.72	0.08
18	0.01	0.50	1.75	0.00
19	0.00	0.05	0.78	0.00
20	0.00	0.00	0.13	0.00
Daily flow rate m^3/day	10.84	33.12	30.95	31.52

Fig. 8 (a)–(d) shows the comparison between the measured and the predicted hourly flow rate one using a conventional model during four specific days. We note that these specific days correspond to the summer and winter solstice days and the vernal and autumnal equinox days. It is found that the

conventional model consistently over-predicts the measurements at all times.
This is expected since the model does not account for local weather conditions such as the presence of cloud and dust.

Moreover, one can observe that there are visible discrepancies between the measurements for the three years. The performance of the conventional model was evaluated in terms of the root mean square error (RMSE). Table X summarizes the RMSE of one year (2010) as well as the global error for the whole samples during the four above mentioned days. It is found that the highest global RMSE is occurred in the autumnal equinox, winter solstice and vernal equinox days with values of 4.26%, 3.7% and 4.34% respectively. This is generally attributed to the local cloud formations in these wintry, autumnally and vernally days which obviously vary from year-to-year.

In contrast, the results presented for the summer solstice day in Fig. 8 (b) show that both the measurements and the conventional model predictions differ only slightly. In fact, there is a practically close agreement between the results of the conventional model and the mean values of the measurements with a slight over- prediction of the hourly flow rate by the conventional model with a global RMSE equal to 1.87%. Results for the other days of the years, which are not presented here follow a similar trend and agree with the above conclusion, i.e. some discrepancies occur among the measurements for different years and with the predictions for the cloudy periods, namely, October–May. These differences decrease obviously for the months of June–September (summer months) for which the sky is relatively clearer.

The promising similarities between the measured and predicted hourly flow rate variations during the clear-sky dates suggest that hourly flow rate have estimated basing on this conventional model. The deviation, though small, is attributed to fluctuations in the solar irradiance and unsteady module temperatures during the measurements.

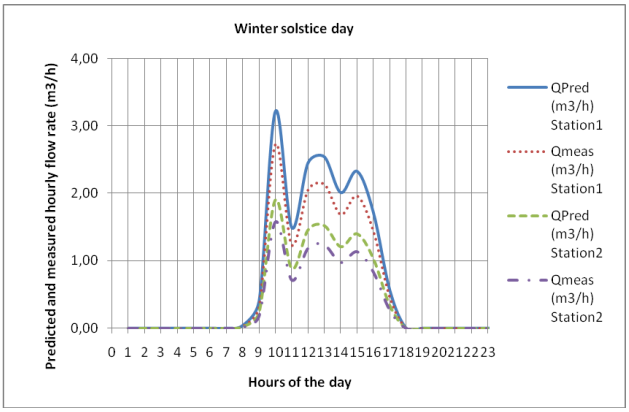

(a)

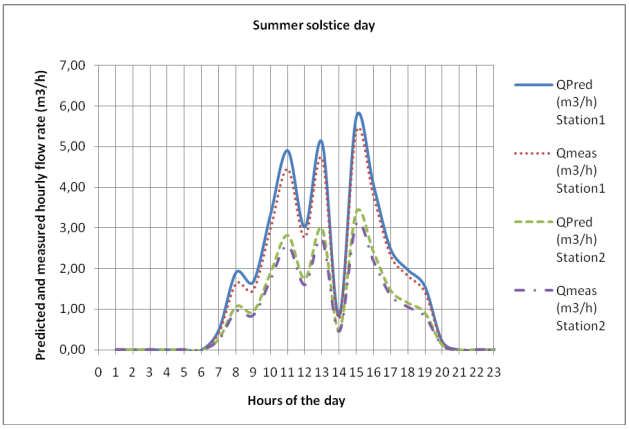

(b)

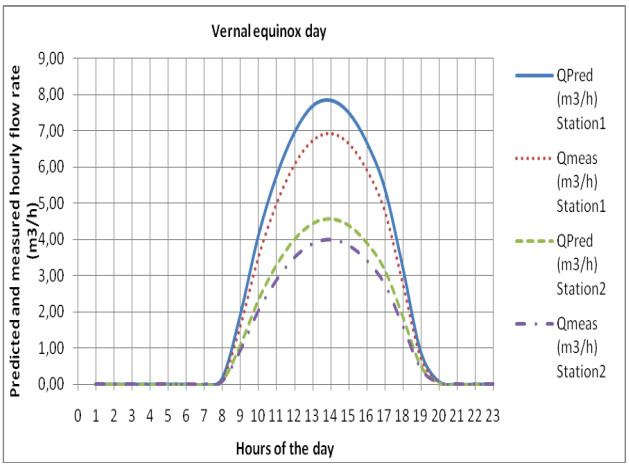

(c)

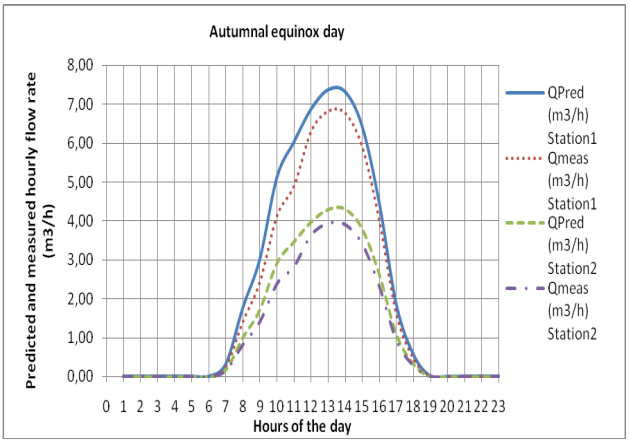

(d)

Fig. 8 Comparison between the predicted and the measured daily flow rate for two stations of PV water pumping during the winter solstice (a), summer solstice (b), vernal equinox (c) autumnal equinox (d) days

TABLE X
ROOT MEAN SQUARE ERROR (RMSE) AGE BETWEEN THE PREDICTED AND THE MEASURED DAILY FLOW RATE

Predicted/Measured daily flow rate	RMSE (%) Station1	RMSE (%) Station 2	Global RMSE (%)
Winter solstice day	3.57	3.83	3.7
Summer solstice day	1.78	1.96	1.87
Vernal equinox day	4.09	4.43	4.26
Autumnal equinox day	4.19	4.49	4.34

V. CONCLUSION

An energy balance model to predict the cell temperature modules of photovoltaic water pumping system was developed and validated using field measurements. The energy balance model considers convection and radiative exchange with the ambient environment as well as conduction through the cover, cell, and the back sheet substrate.

The convection heat loss is predicted using established free and forced convection heat transfer correlations and the radiative heat transfer calculations are based on first principles rather than empirical relations. Both a transient model that accounts for the thermal capacitance and temperature of each material in the cell and a steady energy balance model that creates a thermal resistance network between the cell and ends of the module were developed. In order to quantify variations between predicted and measured values, root mean square error (RMSE) was used. The predicted PV-cell temperatures show good correlation with the measured data with RMSE of 2.6%.

The predicted PV-cell temperatures models were used to predict real-time performance from a PV water pumping systems.

The method has been validated by predicting the performance of two PV water pumping systems in the desert of Medenine (south of Tunisia) during one complete year. The daily flow rate predicted by the method in two stations (Bel Khchab and Om Chraket) have been compared with experimental measurements; the predicted water flow rate shows good agreement with the measured data. A daily comparison basing on the root mean square error showed that this model predicted with good accuracy the real data under the clear sky conditions with an error of 1.87% while its performance decreases in the cloudy conditions with an error reaching the value of 4.34%.

ACKNOWLEDGMENTS

The corresponding author thanks the CRDA of Medenine (Tunisia) for their cooperation. We would like to extend our sincere thanks to Mrs Fadhel Leffet, Mongi Arabi and Cherif Mhemdi for his constructive advice and recommendations given during the execution of the work.

REFERENCES

[1] D.L. King, W.E. Boyson and J.A. Kratochvil, "Photovoltaic Array Performance Model," *Sandia National Laboratories*, Report: SAND2004–3535, 2004.

[2] B.L. Shrestha, E.G. Palomino and G.TamixhMani," Temperature of rooftop photovoltaic modules: Air gap effects," *Proceedings of SPIE*, Vol. 7412, 2009.

[3] M.K. Fuentes, "A Simplified Thermal Model for Flat-Plate Photovoltaic Arrays," *Sandia National Laboratories Report*, SAND85-0330, 1987.

[4] A.D. Jones and C.P. Underwood, "A Thermal Model For Photovoltaic Systems," *Solar Energy*, Vol. 70, no. 4, pp. 349–359, 2001.

[5] M.W. Davis, A.H. Fanney and B.P. Dougherty," Prediction of building Integrated Photovoltaic Cell Temperatures," *ASME Journal of Solar Energy Engineering,* Vol. 123, no. 3, pp. 200–210, 2001.

[6] J.A. Duffie and W.A. Beckman, "Solar Engineering of Thermal Processes," *third ed. John Wiley & Sons Inc*., New York, 2006.

[7] J.A. Del Cueto," Model For The Thermal Characteristics Of Flat-Plate Photovoltaic Modules Deployed At Fixed Tilt," *28th IEEE Photovoltaic Specialists Conference*, 2000, pp. 1441–1445.

[8] S. Krauter, A. Preiss, N. Ferretti and P. Grunow, "PV Yield Prediction for Thin Film Technologies and the Effect of Input Parameters Inaccuracies," *23rd European Photovoltaic Solar Energy Conference*, 2008.

[9] E. Skoplaki, A.G. Boudouvis and J.A. Palyvos, "A simple correlation for the operating temperature of photovoltaic modules of arbitrary mounting," *Solar Energy Materials & Solar Cells*, Vol. 92, pp. 1393–1402, 2008.

[10] E.Skoplaki and J.A. Palyvos, "On the temperature dependence of photovoltaic module electrical performance: A review of efficiency/power correlations," *Solar Energy*, Vol. 83, pp. 614–624, 2009.

[11] Y. Ueda et al., "Performance analysis of various system configurations on grid-connected residential PV systems," *Solar Energy Mater Solar Cells*, Vol. 93, no (6-7), pp.945–949, 2009.

[12] M. Kolhe et al.,"Analytical model for predicting the performance of photovoltaic array coupled with a wind turbine in a stand-alone renewable energy system based on hydrogen," *Renewable Energy*, Vol. 28, no. 5, pp.727–742, 2003.

[13] J.A. Duffie, W.A. Beckman, "Solar engineering of thermal processes," *2nd Edition, New York: Wiley*, 1991.

[14] D.G. Erbs, S.A. Klein and J.A. Duffie, "Estimation of the diffuse radiation fraction for hourly, daily and monthly-average global radiation," *Solar Energy*, Vol. 28, no. 4, pp.293–302, 1982.

[15] D.L. Evans, "Simplified Method for Predicting Photovoltaic Array Output," *Solar Energy*, Vol. 27, no. 6, pp. 555–560, 1981.

[16] J. Royer, T. Djiako, E. Schiller and B.S. Sy," Le pompage photovoltaïque: manuel de cours à l'intention des ingénieurs et des techniciens, "*Institut de l'Énergie des Pays ayant en commun l'usage du Français, Québec, Canada*, 1998.

[17] Ammar Mahjoubi, Ridha Fethi Mechlouch, Ammar Ben Brahim, "Fast and low-cost prototype of data logger for photovoltaic water pumping system," *International Journal of Sustainable Energy*, Vol. 31, no. 3, pp. 189–202, June, 2012.